Alterations in the incisor development in the Tabby mouse

STÉPHANIE MIARD[1], RENATA PETERKOVÁ[2], JEAN-LUC VONESCH[3], MIROSLAV PETERKA[2], JEAN-VICTOR RUCH[1] and HERVÉ LESOT[1*]

[1]INSERM U424, Institut de Biologie Médicale, Faculté de Médecine, Strasbourg, France, [2]Institute of Experimental Medicine, Academy of Sciences of the Czech Republic, Prague, Czech Republic and [3]Institut de Génétique et de Biologie Moléculaire et Cellulaire, Illkirch, France

ABSTRACT **The X-linked tabby *(Ta)* syndrome in the mouse is homologous to the hypohidrotic ectodermal dysplasia (HED) in humans. As in humans with HED, *Ta* mice exhibit hypohidrosis, characteristic defects of hairs and tooth abnormalities. To analyze the effects of *Ta* mutation on lower incisor development, histology, morphometry and computer-aided 3D reconstructions were combined. We observed that *Ta* mutation had major consequences for incisor development leading to abnormal tooth size and shape, change in the balance between prospective crown- and root-analog tissues and retarded cytodifferentiations. The decrease in size of *Ta* incisor was observed at ED13.5 and mainly involved the width of the tooth bud. At ED14.5-15.5, the incisor appeared shorter and narrower in the *Ta* than in the wild type (WT). Growth alterations affected the diameter to a greater extent than the length of the *Ta* incisor. From ED14.5, changes in the shape interfered with the medio-lateral asymmetry and alterations in the posterior growth of the cervical loop led to a loss of the labio-lingual asymmetry until ED17.0. Although the enamel organ in *Ta* incisors was smaller than in the WT, a larger proportion of the dental papilla was covered by preameloblasts-ameloblasts. These changes apparently resulted from reduced development of the lingual part of the enamel organ and might be correlated with a possible heterogeneity in the development of the enamel organ, as demonstrated for upper incisors. Our observations suggest independent development of the labial and lingual parts of the cervical loop. Furthermore, it appeared that the consequences of *Ta* mutation could not be interpreted only as a delay in tooth development.**

KEY WORDS: *incisor, morphogenesis, Tabby mutation, mouse, odontogenesis*

Introduction

Tooth morphogenesis is controlled by continuous and reciprocal epithelio-mesenchymal interactions that involve complex networks of signaling molecules (Maas and Bei, 1997; Thesleff and Sharpe, 1997). Odontogenesis in the mouse is the most frequently used model to study tooth development and the regulatory mechanisms involved. In the mouse, each quadrant comprises one continuously growing incisor, separated from three molars by a long toothless area: the diastema. Differential mitotic activities (Osman and Ruch, 1976; Ahmad and Ruch, 1987; Nso *et al.*, 1992), temporo-spatially defined apoptosis (Lesot *et al.*, 1996; Peterková *et al.*, 1996; Vaahtokari *et al.*, 1996), and changes in cell-cell (Palacios *et al.*, 1995; Obara and Takeda, 1997; Fausser *et al.*, 1998) as well as cell-matrix interactions (Salmivirta *et al.*, 1996; Yoshiba *et al.*, 1998a; Lesot *et al.*, 1999), play important roles in odontogenesis. The number and spatial distribution of functionally differentiated cells (odontoblasts and ameloblasts) determine the final size and shape of the crown.

Abnormalities in the number (hypo- or hyperdontia), size (micro- or macrodontia) and shape of teeth have been well documented in human dental pathology. In most cases, these result from alterations in early tooth development (Ranta, 1988). Autosomal dominant, autosomal recessive or X-linked heredity can lead to more than twenty-five genetic syndromes where dental abnormalities have been observed. Although the genetic basis for such human pathologies has been documented in certain cases (Shapiro and Farrington, 1983), much less information is available on the pathogenesis of tooth development. For this reason, a mouse model appeared to be a potent tool to get information. Several mutant mouse strains (Ta, Tabby; Cr, crinkled; Slk, sleek) express abnormalities of the dentition similar to well known human defects (Sofaer, 1969a,b; 1977). The X-linked tabby *(Ta)* syndrome in the mouse is considered to be homologous to the hypohidrotic ectodermal dysplasia in humans (Weeks and Blecher, 1983; Blecher, 1986). Skin derivatives as well as the dentition are severely affected in patients with ectodermal dysplasia. Besides hypodontia or even anodontia, morphological alterations could affect the
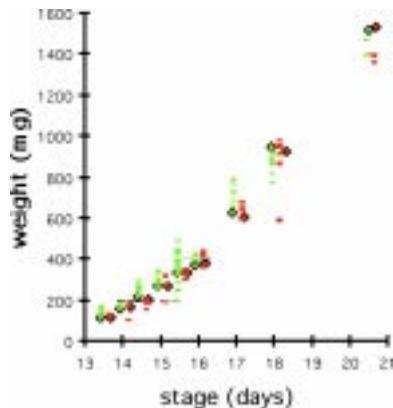
Fig. 1. Weight of WT and *Ta* mouse embryos during development. *For each stage, the weights of the WT were represented in green and those of Ta in red. Diamonds indicate the weights of embryos analyzed in this study.*

existing teeth, which show smaller size and modified shape (Jorgenson, 1980; Crawford *et al.*, 1991). As in humans with ectodermal dysplasia, *Ta* mouse exhibit anhidrosis (absence of sweat glands) as well as characteristic defects of hair and teeth (Grüneberg, 1971; Green, 1981). The third molar may be absent and the first and second molars are reduced in size and their shape is modified. A supernumerary tooth may be present in front of the upper or lower molars. Macrodontia of the first molar as well as hypoplastic, fused or missing incisors have also been reported (Grüneberg 1965, 1966; Sofaer, 1969a,b, 1979; Miller, 1978; Cermaková *et al.*, 1998). *Ta* mouse, therefore, represents a useful tool to analyze mechanisms involved in abnormal development of teeth. A Tabby gene has recently been cloned (Ferguson *et al.*, 1997; Srivastava *et al.*, 1997) and found to encode for a trans-membrane protein, ectodysplasin, whose function has not yet been determined. The Tabby gene was found to be expressed in the outer dental epithelium of developing molar in control but not in *Ta* mutant mice (Srivastava *et al.,* 1997).

The effects of *Ta* Mutation on tooth morphogenesis have been investigated in molars (Sofaer, 1969a). The goal of the present study was to complete this information by analyzing the development of the lower incisor in *Ta* mouse and to compare it to the wild type from the same strain (WT= control). The continuously growing incisor in rodents develops mainly along its antero-posterior axis. Cytodifferentiations lead to development of a distinct labial aspect to the tooth, analogous to the crown of molars, where ameloblasts differentiate and deposit enamel, and the remainder of the tooth where dentin is covered by cementum, similar to the roots of molars. This labio-lingual asymmetry is characteristic of rodent incisors. In order to analyze the consequence of Tabby mutation on incisor development in the mouse, morphometric and histological data were collated using computer-aided 3D reconstructions. *Ta* mutation was found to affect the size of the incisor (diameter and length), its shape and position, as well as cytodifferentiations.

Results

The stage of dental development correlates with body weight of mouse embryos at each chronological stage (Peterková *et al.*, 1993a). To minimize variability of results, paired Tabby *(Ta)* and wild-type (WT) specimens exhibiting the same chronological stage

and similar body weight (diamonds on Fig. 1) were always selected for investigation. Embryos from ED 13.5 were used for this study, up to birth.

Morphometry

During development, the incisor elongated in the posterior direction (compare Figs. 5C, 6C, 7C). At ED 13.5-14.0, the antero-posterior extension of the incisor was the same in control (WT) and *Ta* mouse embryos (Fig. 2A). From ED 14.5, the incisor was shorter in *Ta* than in the WT and this delay in elongation remained at later stages (Fig. 2A).

The diameter of the incisor enamel organ, measured at the posterior three-quarter point of the tooth, rapidly increased up to ED 14.5 both in *Ta* and WT embryos. However, at ED 14.5, the diameter in *Ta* was only 80% of that in WT (Fig. 2B). This difference increased up to ED 16.0 where the diameter in *Ta* was about 50% of that in WT; a value that remained constant up to birth (Fig. 2B and see also Figs. 3,4). The diameter of the papilla was not measured, but 3D reconstructions also clearly showed that it was severely affected as observed at ED 15.5 (Fig. 2B).
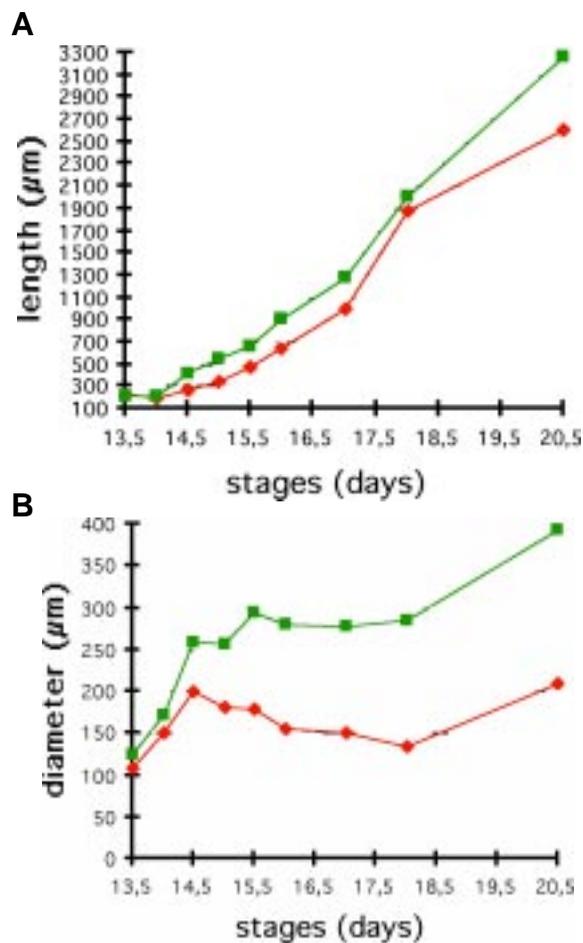
A

B

Fig. 2. Morphometric analysis of the lower incisor development in WT and *Ta* embryos. *The length or antero-posterior extension of the incisor* **(A)** *and the diameter* **(B)** *as measured in the posterior three-quarter point of the tooth has been represented. Data concerning the WT were represented in green and those of Ta, in red.*

Histology

During the period investigated here, the incisor grew actively in a posterior direction. All histological descriptions were performed using sections from the posterior region of the incisor at the three-quarter point of the antero-posterior extension of the tooth.

ED 14.0

At ED 14.0, the incisor was at the bud stage. Cells of the epithelial bud were undifferentiated and condensation of the mesenchyme was still very limited (Fig. 3A,B). No major differences were observed in the *Ta* incisor, except for the smaller medio-lateral width of the epithelial compartment (Compare Fig. 3B to 3A). No enamel knot (EK) could be detected in incisors of WT or *Ta* embryos at ED 14.

ED 15.0

In WT embryos, the incisor had reached the cap stage: the cervical loop (CL) started to develop, thus delimiting the dental papilla although the closure of the CL had not been achieved on the medial side of the incisor (Fig. 3C). Within the enamel organ, the first signs of histogenesis allowed the IDE to be distinguished from the ODE. However, this histogenesis only had a very short antero-posterior extension (155 μm). An EK, which was already present in WT at ED14.5, extending for 120 μm antero-posteriorly, still remained at ED 15.0 but extended for 65 μm only (the histological description and fate of this structure are specified in the accompanying paper Kieffer *et al.,* 1999). An epithelial ridge was observed at the outer surface of the enamel organ on the labial side of the incisor. This had started to protrude towards the peridental mesenchyme (Fig. 3C).

In *Ta* embryos, the size of the enamel organ was much smaller (Fig. 3D) and the shape was also different (Compare Fig. 3C with 3D). The development of the cervical loop was very poor and retarded (not visible on Fig. 3D). The dental papilla had a very small diameter and extended only for 75 μm in the most posterior part of the tooth, instead of 205 μm seen in the WT. The mesenchyme condensed in close proximity to the enamel organ (Fig. 3D).

Histogenesis of the enamel organ had also started in the incisor of *Ta* embryos; however, its antero-posterior extension was limited to 55 μm. Compared to the situation in WT embryos, the appearance of an EK was retarded in the incisor of *Ta* embryos since it became apparent only from ED 15.0. At this stage, the EK extended for 60 μm antero-posteriorly and at ED 15.5, it still extended for 55 μm. The diameter of the EK in the incisor of *Ta* embryos was smaller than that of WT incisors (data not shown).

ED 16.0

Compared to ED 15.0, the shape of the EO was almost maintained (Compare Fig. 3E with 3C) in WT embryos at ED 16.0. However, the diameter of the dental papilla had dramatically increased (Compare Fig. 3E with 3C). On the labial and lingual sides of the incisor, less densely packed cells of the stellate reticulum (SR) were interposed between the ODE and IDE (Fig. 3E) for 545 μm in an antero-posterior direction. The epithelial ridge was more prominent than 24 h earlier (Compare Fig. 3E with 3C).

In the incisors of *Ta* embryos, the enamel organ maintained a size and shape similar to that observed at ED 15.0. The epithelial ridge was present in incisors from *Ta* embryos, but its position was rotated laterally (Fig. 3F). The cell density in the mesenchyme was similar in
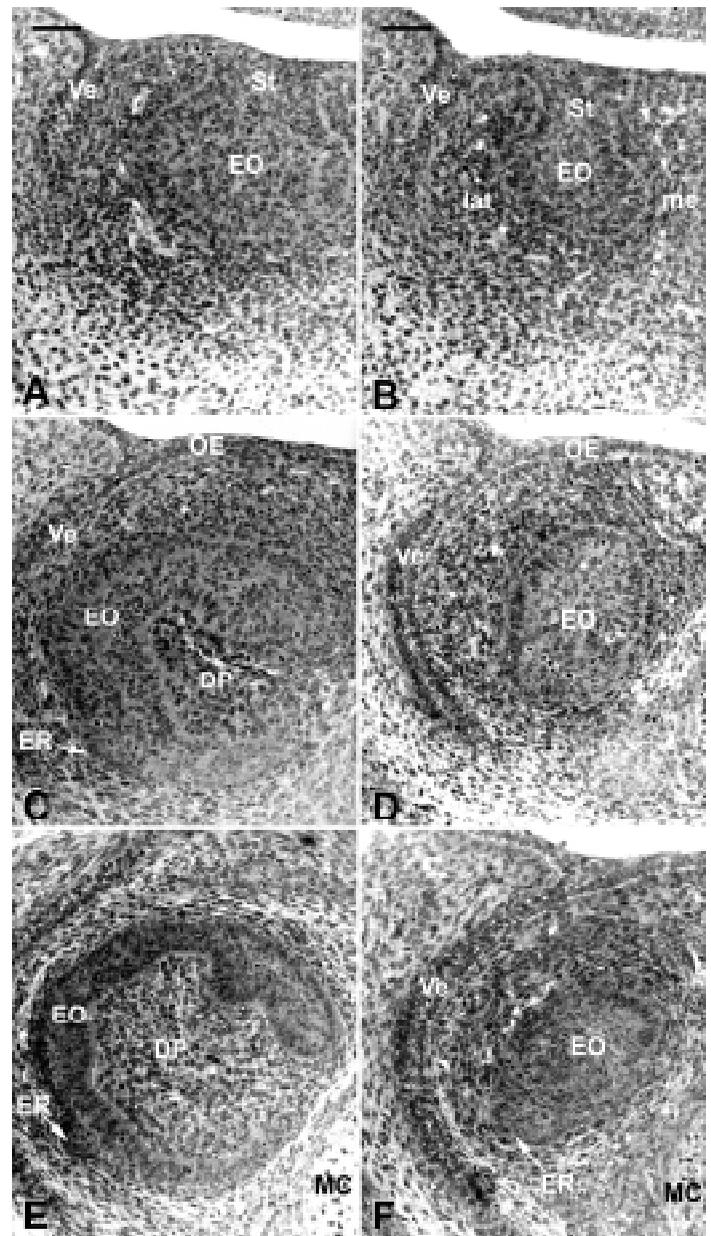

Fig. 3. Frontal histological sections of the lower incisor in WT (A,C,E) and *Ta* (B,D,F) embryos at ED 14.0 (A,B), ED 15.0 (C,D) and ED 16.0 (E,F). *Already at ED 14, the size of the enamel organ (EO) was much smaller in Ta (B) compared to the WT (A). At ED 15, a distinct dental papilla (DP), present in the WT (C), could not be observed in Ta embryos except for a very short segment, more posterior to this section (D). Again at ED 16, the development of the dental papilla was appreciably reduced in Ta embryos (F) compared to WT embryos (E). lat, lateral; me, medial; ER, epithelial ridge; MC, Meckel's cartilage; OE, oral epithelium; St, stalk; Ve, vestibulum. Bar, 50 μm.*

Ta and WT embryos. However, the progressive delimitation of the peridental mesenchyme from the extra-dental mesenchyme was not as marked in *Ta* as in WT (Compare Fig. 3F with 3E). Due to the shorter antero-posterior extension of the dental papilla, the histological section at the posterior three-quarter point of the incisor only went
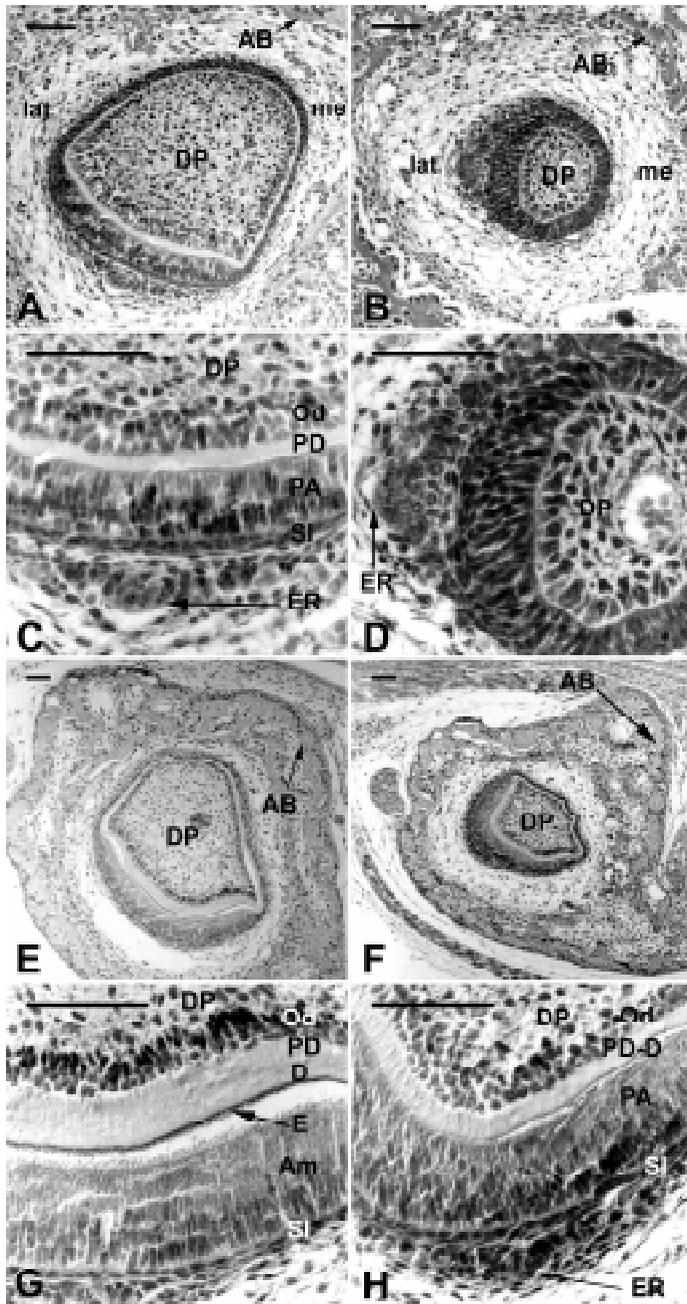
Fig. 4. Frontal histological sections of the lower incisor in WT (A,C,E,G) and *Ta* (B,D,F,H) embryos at ED 18.0 (A,B,C,D) and birth (E,F,G,H). *Low magnifications **(A,B,E,F)** allowed assessment of the size, shape and general histological aspect of the incisor: all three parameters were affected in Ta embryos **(B,F)** when compared to WT **(A,E)**. High magnifications **(C,D,G,H)** illustrated the histogenesis and retarded cytodifferentiations of odontoblasts (Od) and of ameloblasts (Am) in Ta embryos **(D,H)**. At ED 18, predentin (PD) was secreted in WT embryos **(A,C)** but not in Ta **(B,D)** at the same relative position in the incisor. Similarly, at birth, enamel **(E)** was already secreted by ameloblasts (Am) in WT **(G)** but not in Ta **(H)**. AB, alveolar bone; D, dentin; DP, dental papilla; ER epithelial ridge; lat, lateral; me, medial; PA preameloblast; SI, stratum intermedium. Bar, 50 μm.*

through the enamel organ. A short EK (20 μm antero-posteriorly) was maintained in the incisor of *Ta* mice, whilst it had already disappeared in WT. In *Ta*, distinct IDE, SR and ODE were observed for 295 μm antero-posteriorly.

ED18.0

Even in the posterior part of the tooth where sections were analyzed, histogenesis of the EO allowed the IDE, SI and SR to be distinguished on the labial aspect of the incisor in WT embryos (Fig. 4A,C). However, the ODE was more difficult to identify at this stage except in close proximity to the epithelial ridge where it appeared as a single layer of cells (Fig. 4A,C). Functional odontoblasts were observed all around the dental papilla except for a restricted region on the latero-lingual side of the incisor (Fig. 4A) and extended antero-posteriorly for 1020 μm (54% of the length of the pulp). However, the thickness of predentin was greater on the labial aspect of the tooth (Fig. 4A). In the IDE, cells started to elongate (Fig. 4A,C), allowing clear distinction from the shorter cells in the lateral and medial parts of the incisor (Fig. 4A).

In *Ta* embryos, the size of the enamel organ remained very small and its round shape on section was very different from that of the WT (Compare Fig. 4B with 4A). Despite these changes in the shape of the enamel organ, the abnormal position of the epithelial ridge suggested a twist of the incisor around its antero-posterior axis (Fig. 4B). Instead of having a labial position, the epithelial ridge was localized on the lateral side of the incisor in *Ta* embryos (Compare Fig. 4B with 4A). Odontoblasts, which extended for 570 μm (35% of the length of the pulp) antero-posteriorly, appeared as polarized but still very short and not yet functional cells (Fig. 4D). For this reason, the elongation of preameloblasts as observed in the WT (Fig. 4C) was still very poor in *Ta* (Fig. 4D). In *Ta* embryos, the distance between the ODE of the incisor and the alveolar bone appeared to increase compared to the WT (Compare Fig. 4B with 4A).

At birth

In WT newborn mice, functional odontoblasts were present all around the dental papilla (Fig. 4E). On the labial aspect of the incisor, these odontoblasts had deposited a thick layer of predentin-dentin and extended maximally for 2560 μm in an antero-posterior direction (79% of the length of the pulp). In the same region, ameloblasts polarized and elongated (Fig. 4E,G). Functional ameloblasts extended for 1360 μm antero-posteriorly (46% of the length of the pulp). Functional ameloblasts were observed on the medial two-thirds of the crown part of the incisor (Fig. 4G). The epithelial ridge was no longer visible (Fig. 4E).

At this stage, the major differences in the incisor of *Ta* mice were in the size, the shape and the orientation of the tooth, which appeared to be abnormally turned towards the lateral side (Fig. 4F,H). The enamel organ delimited a very small dental papilla, where odontoblasts had differentiated and become functional (Fig. 4H). Functional odontoblasts were observed antero-posteriorly for 1610 μm (67% of the length of the pulp) and functional ameloblasts for 705 μm (29% of the length of the pulp). However, on frontal sections the relative portion of the dental papilla covered by polarized or polarizing cells of the inner dental epithelium appeared increased compared to the WT (Compare Fig. 4F with 4E). This area represented more than a half of the whole dental papilla surface.

Computer-aided 3D reconstructions
Morphological aspects
ED13.5

At ED13.5, the incisor germs were at the bud stage both in WT (Fig. 5A,C,E) and *Ta* (Fig. 5B,D,F) embryos. Medial (Compare Fig.
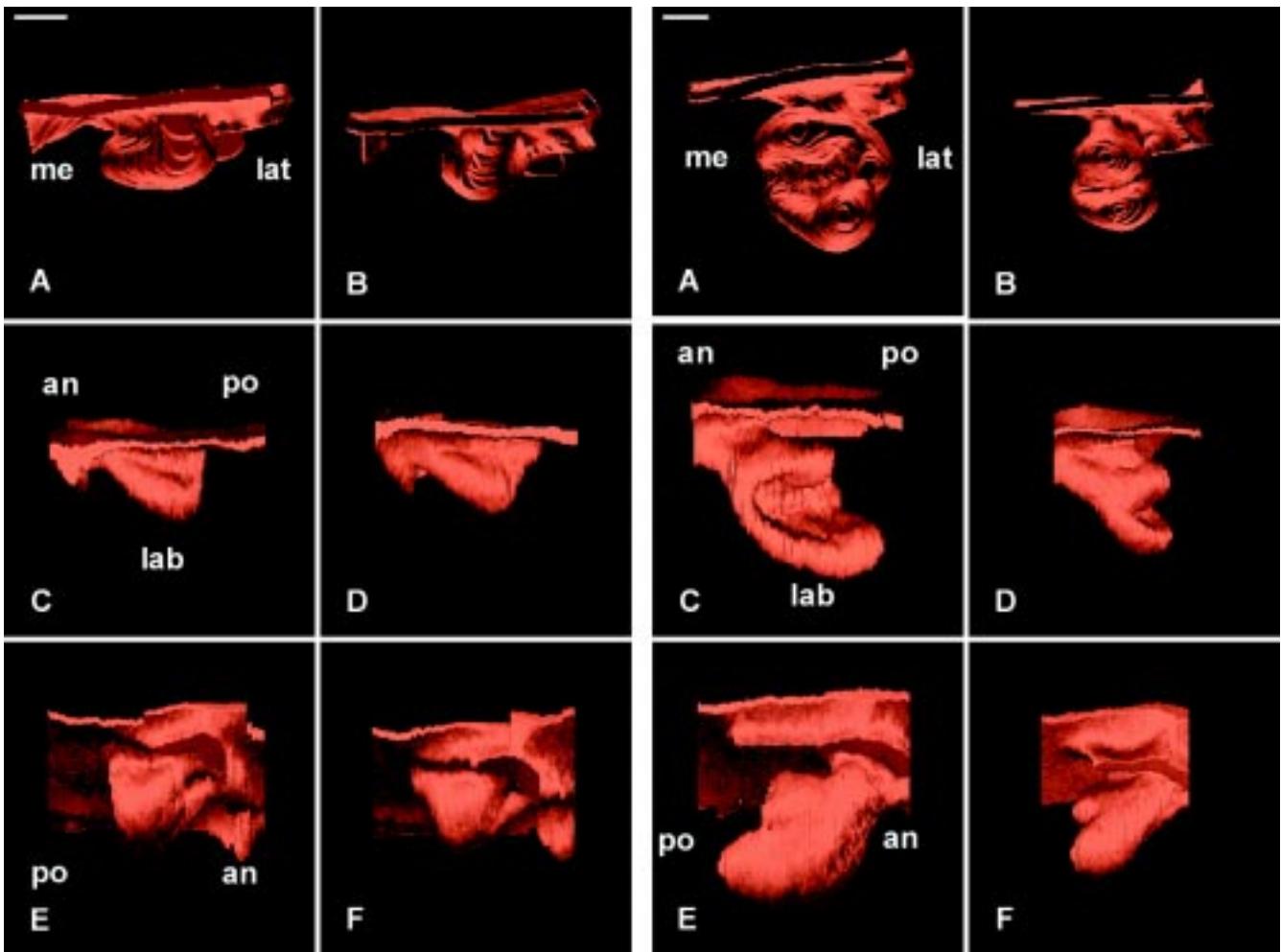
Fig. 5. 3D reconstructions of the dental epithelium of the developing lower incisor in WT (A,C,E) and *Ta* (B,D,F) embryos at ED 13.5 *as seen in posterior* **(A,B)**, *medial* **(C,D)**, *and latero-apical views* **(E,F)**. *The incisor reached the bud stage both in WT* **(A,C,E)** *and Ta* **(B,D,F)** *embryos. The vestibulum was artificially suppressed to facilitate the visualization of the tooth bud. an, anterior; lab, labial; lat, lateral; me, medial; po, posterior. Bar, 100 µm.*

Fig. 6. 3D reconstructions of the dental epithelium of the developing lower incisor in WT (A,C,E) and *Ta* (B,D,F) embryos at ED 14.5 *as seen in posterior* **(A,B)**, *medial* **(C,D)**, *and latero-apical* **(E,F)** *views. The incisor reached the cap stage both in WT* **(A,C,E)** *and Ta* **(B,D,F)** *embryos. However, the development of the cervical loop in WT embryos* **(A,C)** *demonstrated classical labio-lingual and medio-lateral asymmetries. In Ta, the size of the enamel organ was much smaller and changes in the shape also led to loss of asymmetries in the development of the cervical loop* **(B,D,F)**. *The vestibulum was not represented. an, anterior; lab, labial; lat, lateral; me, medial; po, posterior. Bar, 100 µm.*

5C with Fig. 5D) and labio-lateral (Compare Fig. 5E with 5F) views of the buds were very similar in both cases. The only difference was in the medio-lateral width of the bud, which was reduced in the *Ta* embryo (Compare Fig. 5A with 5B). In all reconstructions, at this and later stages, the vestibulum was not represented in order to better visualize the incisor, even in its most anterior region.

ED14.5

The cervical loop developed in the WT (Fig. 6A,C,E) and *Ta* (Fig. 6B,D,F) incisors, which had reached the cap stage. However, 3D reconstructions showed that the size of the enamel organ in *Ta* was considerably reduced compared to the WT (Compare Fig. 6A,C,E with 6B,D,F). Similarly, the cap cavity was much smaller in *Ta* embryos. The development of the cervical loop was much less advanced in *Ta* (Fig. 6B,D,F) compared to WT (Fig. 6A,C,E). Furthermore, the labio-lingual asymmetry in the posterior growth of

the cervical loop was much less apparent in the mutant (Compare Fig. 6D with 6C). However, posterior views of the tooth showed that although the width of the labial part of the cervical loop was maintained in both the mutant and WT incisors, the width of the lingual part of the cervical loop had significantly decreased in *Ta* (Compare Fig. 6B with 6A) and its lateral part was distinct in the WT (Fig. 6A), but not in *Ta* (Fig. 6B).

ED15.5

Both in the WT (Fig. 7C,E) and the mutant (Fig. 7D,F), the development of the cervical loop had progressed. However, the incisor was still at the cap stage (Fig. 7C,D). The closure of the cervical loop on the lateral side had progressed in the WT (Compare Fig. 7C with 6C) and had clearly started with the mutant (Fig. 7D). The labio-lingual asymmetry remained very poor in the *Ta* incisor (Fig. 7D) when compared to the WT (Fig. 7C). The epithelial
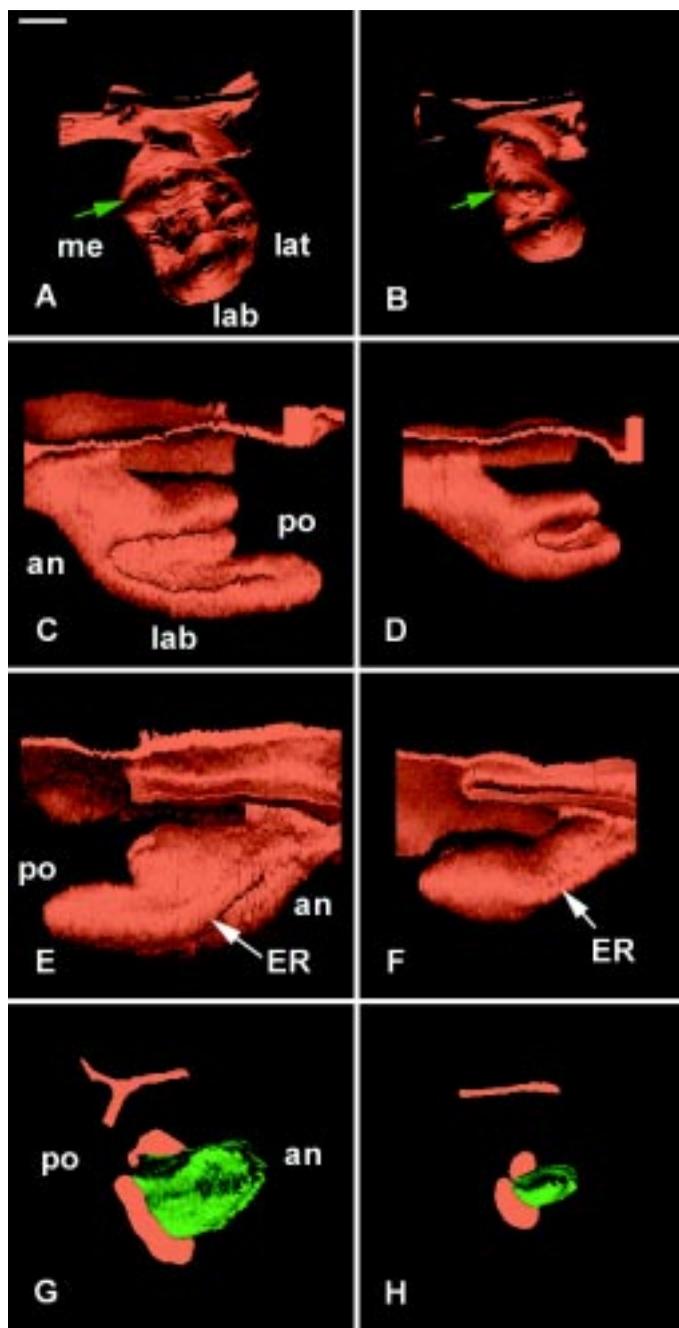
Fig. 7. 3D reconstructions of the dental epithelium (A,B,C,D,E,F) and dental papilla (G,H) of the developing lower incisor in WT (A,C,E,G) and *Ta* (B,D,F,H) embryos at ED 15.5. *The epithelium at the cap stage was seen in posterior* **(A,B)**, *medial* **(C,D)**, *and latero-apical* **(E,F)** *views. The labio-lingual and medio-lateral asymmetries of the developing cervical loop were maintained in WT embryos* **(A,C)**. *In Ta, however, the size of the enamel organ was much smaller* **(B,D,F)** *and changes were observed in the width of the lingual part of the cervical loop (arrow in* **B***) and in the relative posterior extension of the lingual and labial parts of the cervical loop* **(D)**. *Changes in the shape also led to loss of asymmetries in the development of the cervical loop* **(B,D,F)**. *The epithelial ridge (ER) was much more prominent in WT* **(E)** *than in Ta* **(F)** *incisors. The vestibulum was not represented. Ta mutation not only affected the size, but also the shape of the dental papilla* **(G,H)**. *an, anterior; lab, labial; lat, lateral; me, medial; po, posterior. Bar, 100 µm.*

ridge was much more apparent in the posterior part of the incisor in the WT (Fig. 7E) when compared to *Ta* (Fig. 7F). The differences in the size of the incisor between the WT and the mutant were maintained at ED 15.5 (Compare Fig. 7A,E with 7B,F). A similar observation was made when representing the dental papilla (Compare Fig. 7G with 7H). An anterior depression was observed at the tip of the dental papilla in the WT (Fig. 7G) that could be hardly detected in *Ta* (Fig. 7H). Again at ED 15.5, posterior views of the incisors confirmed observations from ED 14.5: the width of the lingual aspect of the cervical loop in *Ta* appeared much more affected than the width of the labial aspect when comparing the mutant to the WT (Compare Fig. 7B with 7A).

ED17.0

At ED 17.0, the cervical loop closed on the medial side and the incisor had reached the bell stage both in the WT (Fig. 8C) and the *Ta* (Fig. 8D). Since ED 15.5, there was a significant increase in the length of the incisor. However, the enamel organ remained shorter in *Ta* embryos (Fig. 8D) and was also much thinner (Fig. 8B) when compared to the WT (Fig. 8C,A). An epithelial ridge was present in both cases (Fig. 8E,F). The diameter of the dental papilla was strongly affected in *Ta* (Fig. 8H) when compared to the WT (Fig. 8G) and the depression at the tip of the dental papilla, well formed in the WT (Fig. 8G), was not visible in the *Ta* (Fig. 8H).

Mitoses and apoptosis

ED 13.5

As mentioned above, the poor condensation of the mesenchyme did not allow clear delimitation of the dental mesenchyme at this stage. For this reason, all metaphases present in the mesenchyme surrounding the epithelial bud have been represented (Fig. 9A,D and 9G,J). The distribution of metaphases appeared homogeneous in both cases (Fig. 9A,D and 9G,J). Apoptosis in the mesenchyme (Fig. 9C,F and 9I,L) was concentrated in two main areas: 1) posteriorly to the tooth bud on the labio-lateral side (Fig. 9C,F) and 2) on a much more medial area close to the Meckel's cartilage (Fig. 9I,L). This pattern was observed in the WT and in the mutant as well (Compare Fig. 9C,I with 9F,L). In the epithelial compartment, metaphases had a ubiquitous distribution in the developing enamel organ in *Ta* (Fig. 9E,K) and in the WT (Fig. 9B,H). Very little apoptosis was observed in the enamel organ; it was concentrated in the oral epithelium. No difference was observed when comparing the situation in *Ta* with that in the WT (Compare Fig. 9E,K with 9B,H).

ED 14.5

At ED 14.5 it was possible to identify cells of the dental mesenchyme due to its condensation; the representation of metaphases was now restricted to this tissue, which was not possible before. Few metaphases were observed in the dental papilla of the WT (Fig. 10A,G) and *Ta* (Fig. 10D,J) incisors. Apoptosis in the mesenchyme was sparse in case of the WT (Fig. 10C,I). In the mutant, apoptotic cells and bodies were still present in the mesenchyme but their number had decreased compared to that at ED 13.5 (Compare Fig. 10F,L with 9F,L). The ubiquitous distribution of metaphases in the developing enamel organ was maintained both for the WT and *Ta* (Compare Fig. 10B,H with 10E,K). At this stage, apoptosis in the epithelial compartment was

concentrated in the stalk and in the oral epithelium (Fig. 10B,H and 10E,K). Both in *Ta* and in the WT, there was a clear cut separation between the stalk, where mainly apoptotic cells and bodies were observed, and the cap of the enamel organ, where most of the cells divided and showed very little or no apoptosis (Fig. 10B,H and 10E,K).

ED 15.5

Again, few metaphases were observed in the dental papilla of WT (Fig. 11A,I) and *Ta* (Fig. 11E,M) incisors. Sparse apoptosis was observed in the mesenchyme of both the WT (Fig. 11C,L) and mutant mice (Fig. 11G,O). The ubiquitous distribution of metaphases in the developing enamel organ was maintained both for the WT and *Ta* (Compare Fig. 11B,J with 11F,N). Apoptotic cells and bodies in the epithelial compartment were still concentrated in the stalk and in the oral epithelium (Fig. 11B,J and 11F,N). However, their amount strongly decreased when compared to that at ED 14.5 (Compare Fig. 11B,J with 10B,H). The same situation was observed in *Ta* and in the WT (Compare Fig. 11F,N with 10E,K). A clear-cut separation, between the stalk where apoptosis was concentrated and the enamel organ where the mitotic activity was prominent, was maintained in both the WT (Compare Fig. 11B,J with 10B,H) and the mutant (Compare Fig. 11F,N with 10E,K). Apoptosis in the enamel organ remained distant from the epithelio-mesenchymal junction at the tip of the dental papilla in the WT as well as in *Ta* embryos (Compare Fig. 11D,K with 11H,P).

ED 17.0

Metaphases were mainly detected in the posterior half of the dental papilla in the WT (Fig. 12A) although they maintained a ubiquitous distribution in the dental mesenchyme of *Ta* incisor (Fig. 12E). Similar to what was observed at ED 15.5, sparse apoptotic cells and bodies were found in the mesenchyme (Fig. 12C,G,K,O). The number of metaphases in the dental mesenchyme remained low in both cases (Fig. 12A,E,I,M). A ubiquitous distribution of metaphases in the enamel organ was observed in the *Ta* (Fig. 12F,N) and in the WT (Fig. 12B,J). However, their visualization associated with the representation of the mesenchyme (Fig. 12D,H,L,P) indicated that the most anterior part of the enamel organ on its labial side was almost devoid of metaphases in the WT (Fig. 12D,L) but not in the *Ta* (Fig. 12H,P). Very few metaphases were observed in the stalk where apoptosis was prominent: this was observed both in
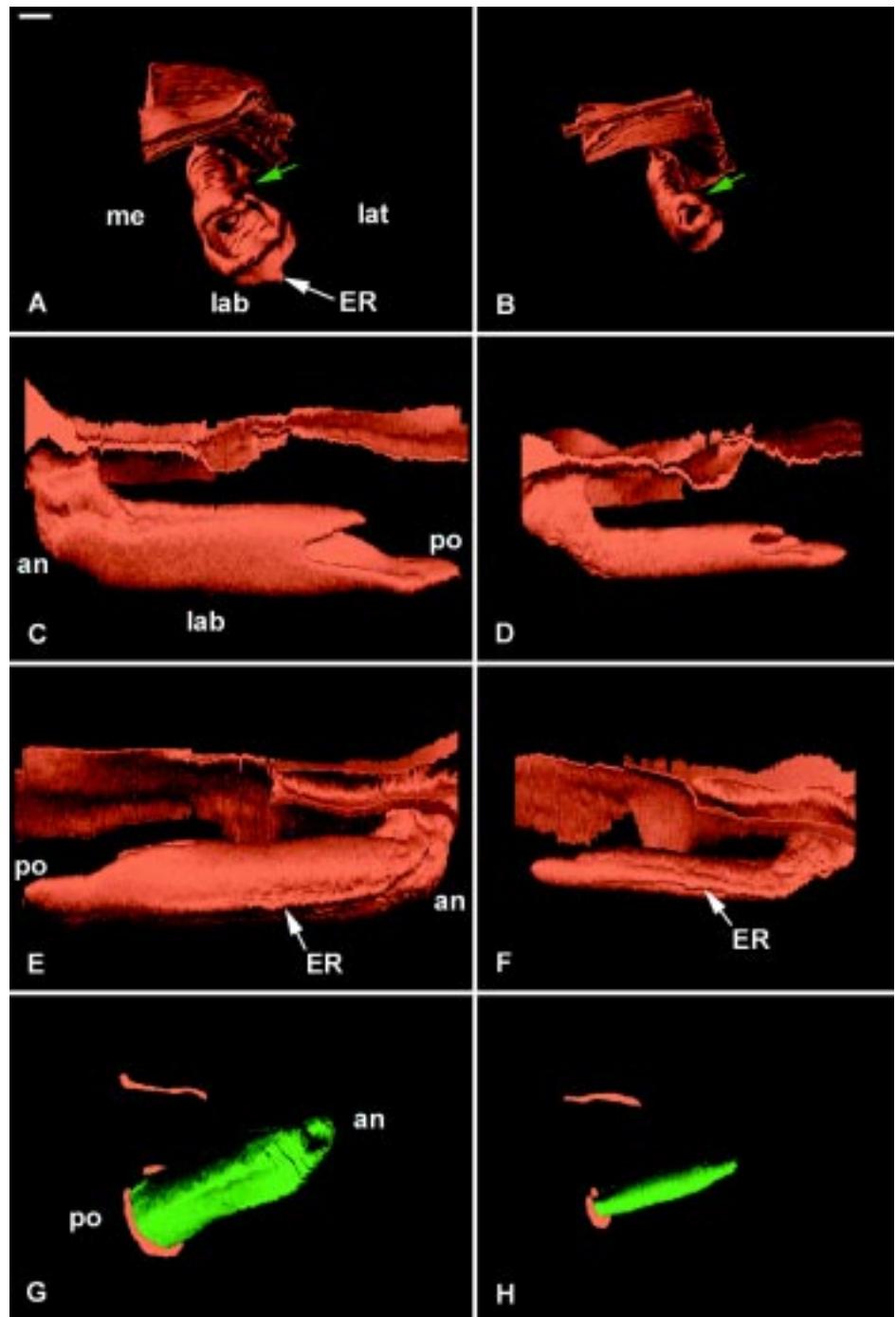

Fig. 8. 3D reconstructions of the dental epithelium (A,B,C,D,E,F) and dental papilla (G,H) of the developing lower incisor in WT (A,C,E,G) and *Ta* (B,D,F,H) embryos at ED 17.0. *The epithelium at the cap stage was seen in posterior* **(A,B)**, *medial* **(C,D)**, *and latero-apical* **(E,F)** *views. Medio-lateral asymmetries of the developing cervical loop (CL) were observed in incisor from WT* **(C)** *and from Ta* **(D)** *embryos. In Ta, however, the size of the enamel organ remained much smaller* **(B,D,F)** *than in the WT* **(A,C,E)** *and changes were observed in the width of the lingual part of the cervical loop (green arrow in* **B**). *The vestibulum was not represented. The size of the dental papilla (represented in green) in Ta embryo* **(H)** *was strongly reduced as compared to that in the WT* **(G)**. *an, anterior; ER, epithelial ridge; lab, labial; lat, lateral; me, medial; po, posterior. Bar, 100 μm.*

incisors from the WT (Fig. 12B,J) and the mutant (Fig. 12F,N). Apoptosis in epithelium came much closer to the epithelio-mesenchymal junction in the WT (Fig. 12D) than in the mutant (Fig. 12H).
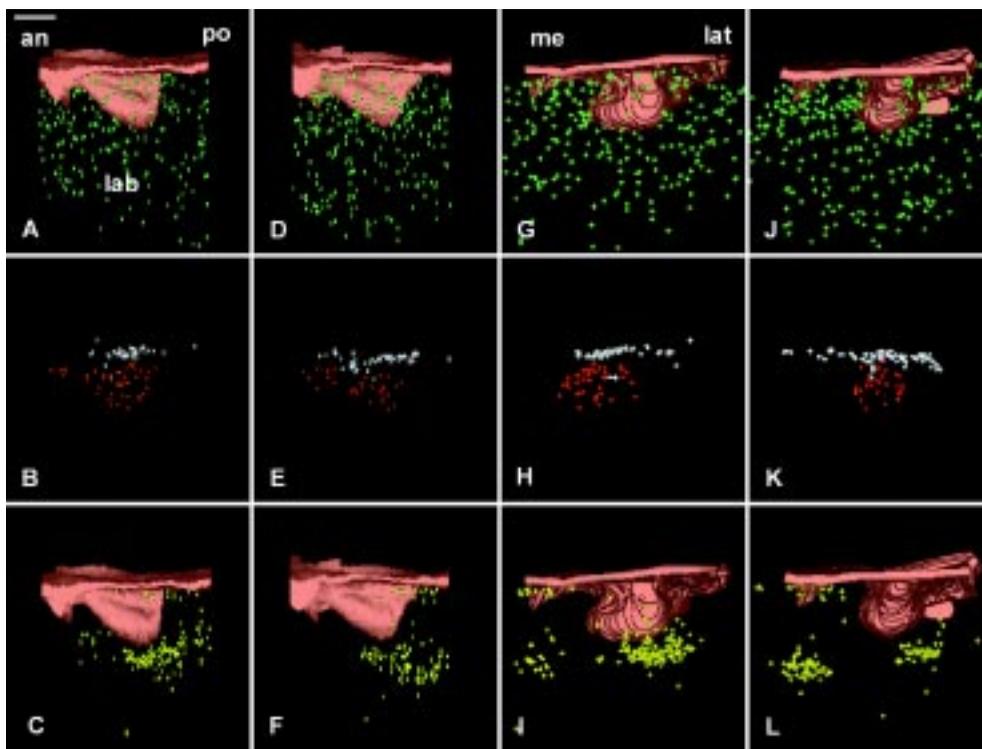
Fig. 9. 3D distribution of mitoses and apoptoses in the incisor at ED 13.5 of WT (A,B,C,G,H,I) and *Ta* (D,E,F,J,K,L) embryos. *The enamel organ was seen in medial (A-F) and posterior (G-L), views. Metaphases in the dental mesenchyme were visualized as green dots (A,D,G,J), in the dental epithelium as red dots (B,E,H,K) and apoptotic bodies and cells in the mesenchyme as yellow dots (C,F,I,L) and in the epithelium as white dots (B,E,H,K). Apoptotic cells and bodies in the mesenchyme were associated with the Meckel's cartilage in the most medial part of the reconstruction (I,L) and more laterally were located under the dental bud (I,L). In this latter case, they were concentrated mainly under the posterior half of the bud (C,F). Apoptosis in the epithelium was localized along the surface in contact with the oral cavity (B,E,H,K). Mitoses in the mesenchyme (A,D,G,J) and in the epithelium (B,E,H,K) had a ubiquitous distribution. The localizations of these cellular events were very similar in the developing incisor of WT and Ta embryos. an, anterior; lab, labial; lat, lateral; me, medial; po, posterior. Bar, 100 µm.*

Apoptosis was observed in the epithelial ridge in the WT (Fig. 12J) but not in the *Ta* (Fig. 12N).

Discussion

The present study has shown that the *Ta* mutation has major consequences for the morphogenesis of incisors, starting early during embryonic development. Abnormalities were related to the size and shape of the tooth, as well as to the balance between prospective crown- and root-analog tissues, and to cytodifferentiations, which were retarded in *Ta* animals.
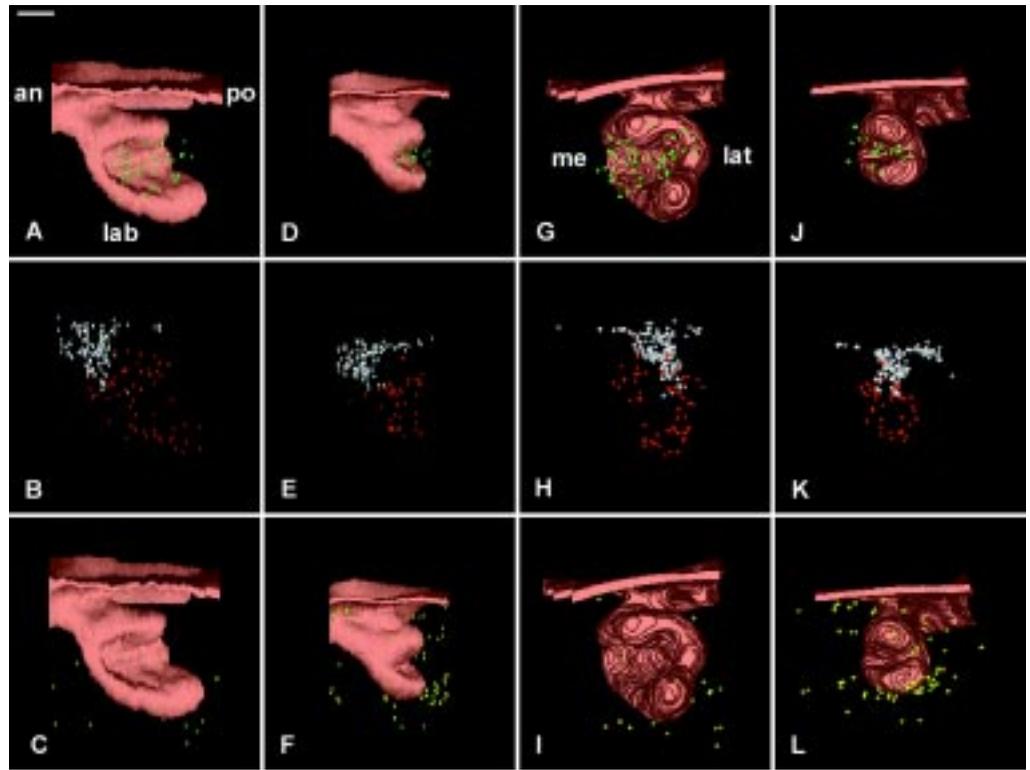
Size

Attempts were made to better evaluate the consequence of *Ta* mutation on incisor growth by measuring its diameter on frontal section at a fixed point along the antero-posterior axis (i.e. the posterior three-quarter point of the incisor), and also the length of the tooth. Since the diameter varies along the antero-posterior axis of the tooth, 3D reconstructions appeared to be much more representative of changes. This approach clearly showed that the decrease in the size of the incisor in *Ta* mouse was already visible at ED 13.5 and mainly involved the width of the tooth bud. However, this difference between *Ta* and WT became more marked at later stages of development. At later stages, the incisor was shorter and narrower in *Ta* than in WT embryos. Alterations in the growth of incisors in *Ta* embryos apparently affected the diameter to a greater extent than the length of the tooth germ. The spatial distribution of metaphases did not show any difference when comparing *Ta* to WT. However, this approach was not quantitative; more subtle difference, such as a lengthening of the cell cycle, might be responsible for the smaller size of the tooth germ in *Ta* embryos. This hypothesis will have to be tested by analysis of

kinetics similar to those experiments performed in the molar (Coin *et al.*, 1999).

A possible relationship between *Ta* mutation and EGF-related disorders has been suggested (Blecher *et al.,* 1983, Robertson and Blecher, 1987). A significant decrease in size of the submandibular gland and delay in the development of the granular convoluted tubules, which normally release EGF, have been found in mutant mice (Blecher *et al.,* 1983; Isaacs *et al.*, 1998). The timing of incisor eruption is significantly delayed in *Ta* mice and this delay could be reversed by injection of EGF to neonatal hemizygote and homozygote *Ta* mice (Kapalanga and Blecher, 1990). EGF and EGFr are expressed in the mouse embryonic first branchial arch and its derivatives from ED 9 through ED 15 (Nexo *et al.*, 1980; Kronmiller *et al.*, 1991a; Shum *et al.*, 1993) and EGF is known to regulate tooth development during this period (Kronmiller *et al.*, 1991b; Hu *et al.*, 1992). Blocking EGF in cultured E10 mandibular arches (Shum *et al.*, 1993) or blocking a kinase activity associated with EGFr (Hu *et al.*, 1992) resulted in a decrease in tooth bud size and alterations in its shape. More recently, hypohidrotic ectodermal dysplasia and *Ta* phenotypes have been suggested to show a strong decrease in EGFr expression (Vargas *et al.*, 1996), but again information is lacking as to whether this expression pattern pre-exists in embryonic tissues, and more specifically in the developing incisor.

Apoptosis in the mesenchyme and in the epithelium was not significantly affected in *Ta* embryos. In the developing lower incisors of both *Ta* and WT embryos, apoptosis concentrated in similar areas (i.e. in the stalk and oral epithelium as well as posteriorly to the labial aspect of the cervical loop and in a more medial region of the mesenchyme). These areas exhibiting high apoptosis were similar to those reported during incisor development in ICR mouse (Kieffer *et al.*, 1999).

Fig. 10. 3D distribution of mitoses and apoptoses in the incisor at ED 14.5 of WT (A,B,C,G,H,I) and *Ta* **(D,E,F,J,K,L) embryos.** *The enamel organ was seen in medial* **(A-F)** *and posterior* **(G-L)**, *views. Metaphases in the dental mesenchyme were visualized as green dots* **(A,D,G,J)**, *in the dental epithelium as red dots* **(B,E,H,K)** *and apoptotic bodies and cells in the mesenchyme as yellow dots* **(C,F,I,L)** *and in the epithelium as white dots* **(B,E,H,K)**. *At this stage, it was possible to distinguish the dental papilla from surrounding mesenchyme. Compared to the situation at ED13.5, the number of apoptotic cells and bodies in the mesenchyme were appreciably decreased at ED 14.5* **(C,F,I,L)**. *Much fewer were observed in the WT* **(C,I)** *than in Ta* **(F,L)**. *Apoptosis in the epithelium was still localized along the surface in contact with the oral cavity, but also in the stalk* **(B,E,H,K)**. *Mitoses in the mesenchyme* **(A,D,G,J)** *had a ubiquitous distribution. In the epithelium, mitoses were observed in the dental epithelium, whilst apoptotic figures were concentrated in the stalk* **(B,E,H,K)**. *an, anterior; lab, labial; lat, lateral; me, medial; po, posterior. Bar, 100 μm.*

Shape

Ta incisors not only demonstrated change in their size, but also in their shape. These changes in the shape were already visible at ED 13.5, when the epithelial bud appeared not to be as wide in *Ta* embryos as in the WT. This situation was maintained at later stages, although it also involved the height and length of the tooth germ and thus had more to do with a general decrease in size. Changes interfering with the labio-lingual asymmetry were detected from ED 14.5. Two distinct observations could be made. First, the antero-posterior growth of the cervical loop was altered, since up to ED 15.5 the cervical loop had approximately the same posterior extension on the labial and lingual side in *Ta* embryos instead of a clear asymmetry as in the WT. Second, the width of the lingual part of the cervical loop was much reduced in *Ta* embryos compared to the width of the labial one. These observations suggested that the development of the cervical loop on the labial and lingual aspects of the incisor was independent, or at least there appeared to be distinct consequences for the *Ta* mutation on both sides. Retinoic acid has been reported to play a role in the labio-lingual asymmetrical development of the incisor at ED 14 (Bloch-Zupan *et al.*, 1994).

Our observations further suggest that the consequences of *Ta* mutation cannot be interpreted only as a delay in development, as reported for the basal layer of the skin (Vielkind and Hardy, 1996). At later stages, shortly after birth, there were obvious modifications in the crown-analog/root-analog proportions. Examination of frontal sections indicated that, despite the slightly smaller size of the incisor enamel organ in newborn Ta mice, elongated inner dental epithelial cells, which would later give rise to ameloblasts, covered a larger proportion of the dental papilla. This was confirmed by the examination of postnatal specimens (data not shown). These changes in the crown-analog/root-analog proportions might result from the reduced width of the lingual part of the cervical loop as observed from ED 14.5 and the virtual absence of the lateral element of the cervical loop at ED 14.5. The development of this lateral part of the cervical loop was found to start as a distinct bulge part on the dental epithelium at ED 13.5 in ICR mice, whose shape became progressively less and less marked from ED 14.0 (Kieffer *et al.*, 1999). Experimental approaches have shown that the dental mesenchyme at the cap stage controls tooth morphogenesis (Kollar and Baird 1969; 1970; Schmitt *et al.*, 1999). Similar experiments will have to be performed with the WT/*Ta* incisor tissues to test whether different domains may exist in the epithelial compartment of the incisor at the cap stage. Such a hypothesis might be supported by the developmental heterogeneity of the upper incisor enamel organ (Peterková *et al.*, 1993b).

At ED 15.5 and later, the shape of the mesenchyme at the tip of the developing incisor of *Ta* mice was different from that observed in the WT tooth. This morphological difference might result from absence of reactivation of mitosis in the central part of the EK (Coin *et al.*, 1999). The presence of an enamel knot was detected in the incisor of the WT and *Ta* embryos, similar to that described in more detail in the ICR strain (Kieffer *et al.*, 1999). However, compared to the WT, the enamel knot in the incisor of *Ta* embryos appeared at a later stage, was smaller, and also disappeared later.

Cytodifferentiations

Compared to that of the WT, the developing incisor in *Ta* embryos showed a marked displacement of the epithelial ridge around the antero-posterior axis at ED 15.0-15.5. However, posterior views of 3D reconstructions did not show a twist of the whole incisor enamel organ at these stages. At later stages, ameloblasts
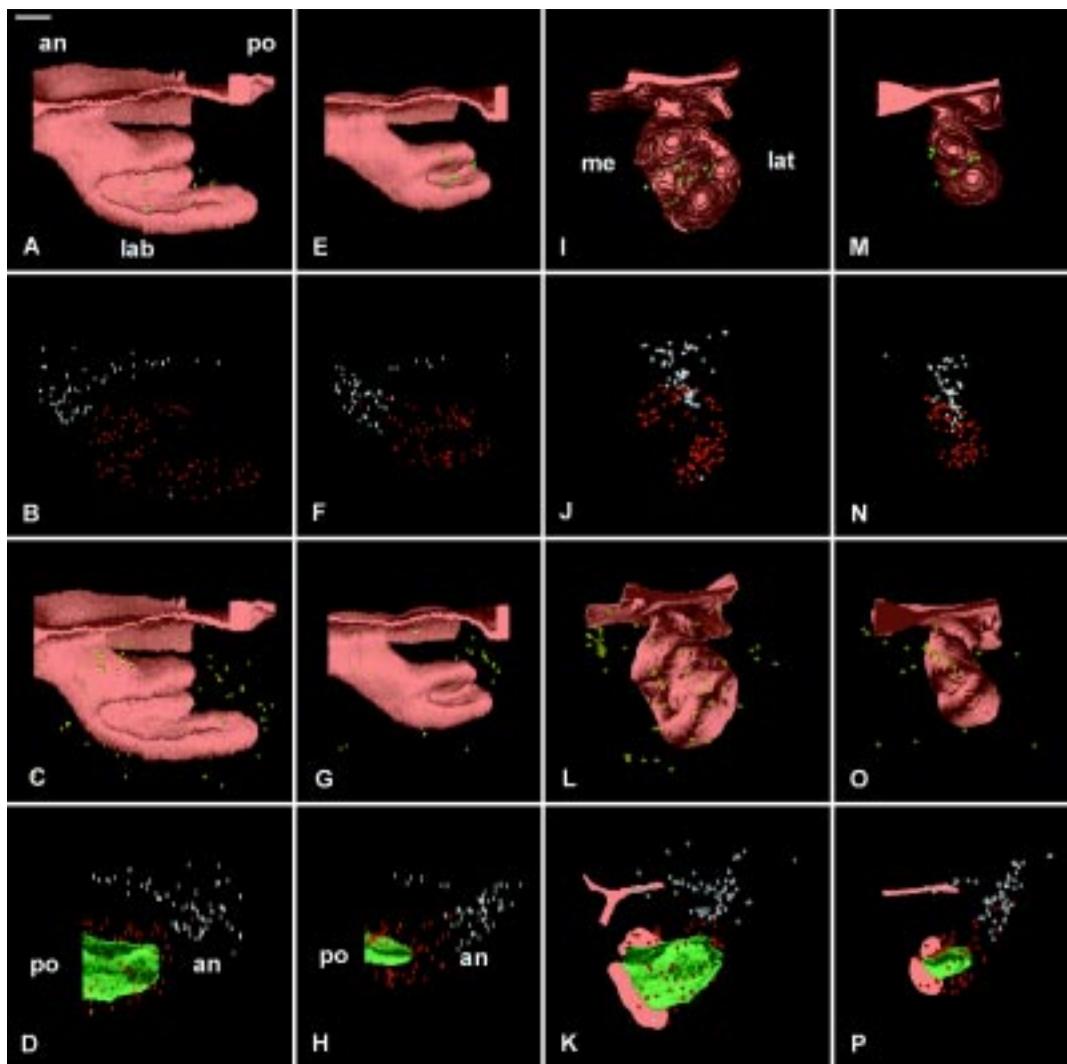
Fig. 11. 3D distribution of mitoses and apoptoses in the incisor at ED 15.5 of WT (A-D,I-K) and *Ta* (E-H,M-P) embryos. *The enamel organ was seen in medial **(A-C,E-G)** and posterior **(I-L,M-O)** views. Metaphases in the dental mesenchyme were visualized as green dots **(A,E,I,M)**, in the dental epithelium as red dots **(B,F,J,N)** and apoptotic bodies and cells in the mesenchyme as yellow dots **(C,G,L,O)** and in the epithelium as white dots **(B,D,F,H,J,K,N,P)**. The dental papilla, represented in green, was much smaller in Ta **(H,P)** embryos than in WT **(D,K)**. Lateral views demonstrated that apoptosis in the epithelium always remained at a long distance from the dental papilla **(D,H)**. an, anterior; lab, labial; lat, lateral; me, medial; po, posterior. Bar, 100 μm.*

were covering the labial surface of the developing tooth in WT embryos although they were localized on a more lateral position in the incisor of *Ta* embryos. This twist progressively increased antero-posteriorly (i.e. when the development proceeded). This abnormality might be correlated with the fact that the surface covered by the root-analog part of the incisor was appreciably reduced in *Ta* mutants leading to a decrease in the anchoring system of the root-like surface. This might also be correlated with the increased space that exists in between the incisor and the alveolar bone.

Odontoblasts are present all around the epithelio-mesenchymal junction in rodent incisors, although ameloblasts differentiate in a more restricted area on the labial side (Cohn, 1957; Warshawsky, 1968). Both the labial and lingual incisor predentin can promote the cytological and functional differentiation of competent preameloblasts in molar teeth (Amar *et al.*, 1986, 1989). The absence of functional ameloblasts on the lingual side of mouse incisor was thus suggested to result from a lack of competence of the cells of the IDE. On the lingual side, IDE cells might withdraw from the cell cycle earlier than on other aspects of the incisor, probably before achievement of the minimal number

of divisions required for their acquisition of competence to respond to specific epigenetic control mechanism (Ruch, 1990; Nso *et al.*, 1992). Heterotopic associations of labial IDE cells with lingual predentin-dentin or of lingual IDE cells with labial predentin-dentin did not lead to change in the original fate of IDE cells, suggesting an endogenous control mechanism for cell kinetic parameters (Amar *et al.*, 1989). Although on frontal sections, the surface of the dental papilla covered by ameloblasts proportionally increased in *Ta* embryos, the antero-posterior extension of functional cells was much shorter. In fact, this apparently resulted from two independent mechanisms. A delay in tooth development might be responsible for the shorter antero-posterior extension of odontoblast and ameloblast differentiation, whilst the change in balance of crown-/root-analog parts might result from preferential decrease in the development in width of the lingual aspect of the cervical loop.

Among constituents that might control the differentiation pathway of IDE cells, the basement membrane has been shown to display labio-lingual specificities (Bloch-Zupan *et al.*, 1994; Meyer *et al.*, 1995; Yoshiba *et al.,* 1998b). The presence of laminin-5 on the lingual side or its absence on the labial side demonstrated
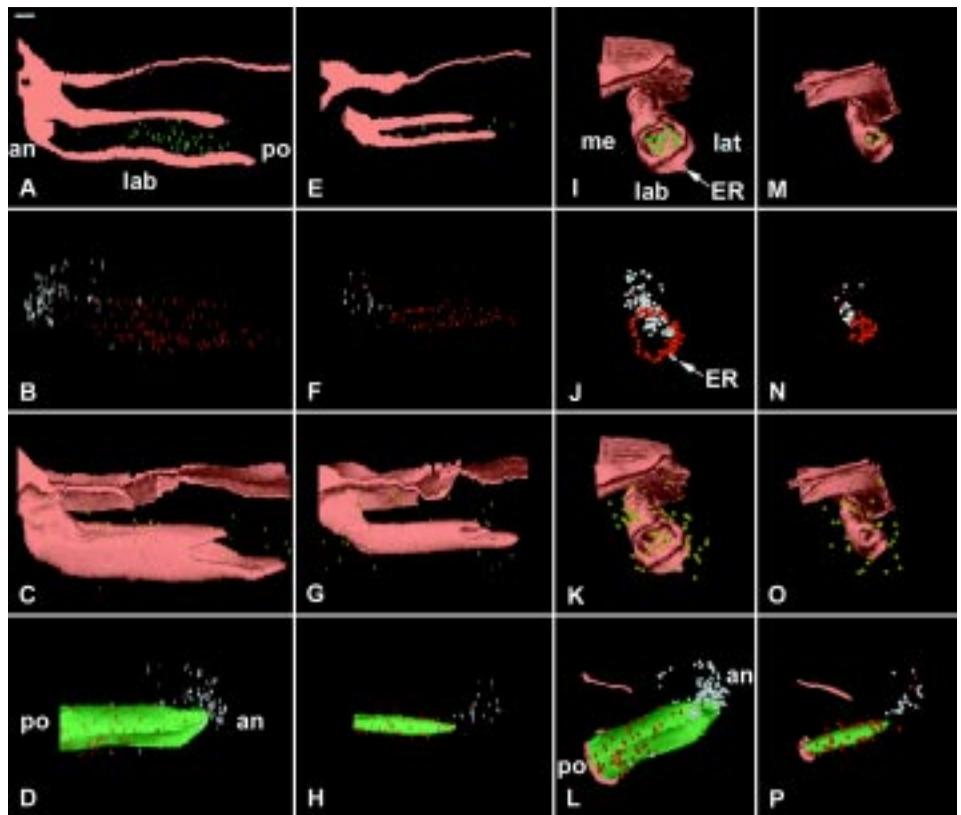
Fig. 12. 3D distribution of mitoses and apoptoses in the incisor at ED 17.0 of WT (A-D,I-L) and *Ta* **(E-H,M-P) embryos.** *The enamel organ was seen in medial* **(A-C,E-G***) and posterior* **(I-K,M-O)** *views. Metaphases in the dental mesenchyme were visualized as green dots* **(A,E,I,M***), in the dental epithelium as red dots* **(B,F,J,N)** *and apoptotic bodies and cells in the mesenchyme as yellow dots* **(C,G,L,O)** *and in the epithelium as white dots* **(B,D,F,H,J,K,N,P)**. *The dental papilla was represented in green* **(D,H,L,P)** *and the most posterior section in orange allowed to visualize the position of the oral epithelium for orientation. an, anterior; lab, labial; ER, epithelial ridge; lat, lateral; me, medial; po, posterior. Bar, 100 µm.*

changes in the composition of the basement membrane itself (Yoshiba *et al.,* 1998b). Furthermore, the existence of single (on the lingual side) or multiple superimposed (on the labial side) basal laminae in the region of the cervical loop, reflected either qualitative differences in IDE cell-basal lamina interactions or differences in the metabolic and mitotic activities of these cells (Meyer *et al.,* 1995). Further investigations will have to be performed to determine which of these parameters were modified as a result of the *Ta* mutation.

Materials and Methods

Mice

All animals were segregated from the inbred tabby line B6CBACa-A^{W-J}/A-Ta/0. The breeder pairs were purchased from the Jackson Laboratory, USA.

Tabby mutant mice

The tabby phenotypes of the mice were determined according to external criteria (Green, 1981). The *Ta*-homozygous females and *Ta*-hemizygous males and females exhibited an identical tabby phenotype. For this reason, the *Ta/Ta* and *Ta/*0 females were combined in a unit group indicated as *Ta*-homozygous/hemizygous females (Cermáková *et al.,* 1998). These females were mated with their relatives (*Ta/*0) hemizygous males X/Y and their offspring were harvested and identified as *Ta* embryos/foetuses in the text.

Wild-type mice

The males and females were generated by inbreeding of wild type brothers and sisters of mutant animals (Cermáková *et al.,* 1998). All these animals exhibited a normal, non-tabby phenotype and their offspring were harvested and identified as wild-type (WT) embryos/foetuses in the text.

Harvesting and staging of embryos

The mice were mated overnight. The midnight before morning detection of the vaginal plug was determined as the embryonic day (ED) 0.0 for chronological staging of offspring. The embryos and foetuses were harvested at noon and midnight from ED 12.5 to 18. Newborn mice (20.5 days after conception) were also used to examine cytodifferentiations. The chronological stage of specimens was specified by their wet body weight (Peterková *et al.,* 1993a). The specimens weighing up to 500 mg were distributed in 25 mg weight classes (wtc.), up to 1000 mg in 50 mg classes and embryos weighing more than 1000 mg were distributed in 100 mg weight classes. In total, 61 *Ta* and 113 WT embryos were fixed in Bouin-Hollande fluid. One specimen from each weight class at each chronological stage was chosen and its head processed for histology.

Histology

Five µm frontal serial sections from paraffin embedded heads were stained with alcian blue-hematoxylin-eosin.

Mitoses and apoptosis

When representing mitoses, only metaphases were taken into account. Mitoses in the dental mesenchyme included those present in the dental papilla and the condensed part of the dental sac (Lesot *et al.,* 1996). At early stages, when the condensation of the mesenchyme was not sufficient to allow objective identification, all metaphases present in the mesenchyme surrounding the dental bud were represented.

Apoptotic cells and bodies were identified from histological sections on the basis of morphological criteria (Kerr *et al.,* 1995, Turecková *et al.,* 1996); their nature has previously been confirmed using the TUNEL method

(Turecková *et al.*, 1996). At ED 17.0, keratinization of the oral epithelium had started; apoptosis related to this process (Schwartz and Osborne, 1995) was not represented.

Morphometry

The length of the enamel organs was estimated by counting the number of frontal sections (5 μm thickness) where the incisor was present. The diameter was measured at a fixed point, three-quarter of the total length of the incisor in the posterior part, from drawings made with a drawing chamber.

3D reconstructions

The contours of the mandibular dental and oral epithelium were drawn from serial histological sections (5 μm intervals) using a Zeiss microscope equipped with a drawing chamber at a magnification of 320x. Mitoses and apoptotic figures were recorded in the dental epithelium and mesenchyme. The digitalization of the serial drawings and correlation of successive images (Olivo *et al.*, 1993) have been previously described (Lesot *et al.*, 1996). Software packages allowing image acquisition and treatment were developed and adapted to this work. Three-dimensional images were generated using a volume-rendering program (Sun Voxel, Sun Microsystems).

References

AHMAD, N. and RUCH, J.V. (1987). Comparison of growth and cell proliferation kinetics during mouse molar odontogenesis *in vivo* and *in vitro*. *Cell. Tissue Kinet. 20*: 319-329.

AMAR, S, LUO, W, SNEAD, M.L. and RUCH, J.V. (1989). Amelogenin gene expression in mouse incisor heterotopic recombinations. *Differentiation 41*: 56-61.

AMAR, S., KARCHER-DJURICIC, V., MEYER, J.M. and RUCH, J.V. (1986). The lingual (root analogue) and the labial (crown analogue) mouse incisor dentin promotes ameloblast differentiation. *Arch. Anat. Microsc. Morphol. Exp. 75*: 229-239.

BLECHER, S.R. (1986). Anhidrosis and absence of sweat glands in mice hemizygous for the Tabby gene: supportive evidence for the hypothesis of homology between Tabby and human. *J. Invest. Dermatol. 87*: 720-722.

BLECHER, S.R., DEBERTIN, M. and MURPHY, J.S. (1983). Pleiotropic effect of Tabby gene on epidermal growth factor-containing cells of mouse submandibular gland. *Anat. Rec. 207*: 25-29.

BLOCH-ZUPAN, A., MARK, M.P., WEBER, B. and RUCH, J.V. (1994). In vitro effects of retinoic acid on mouse incisor development. *Arch. Oral Biol. 39*: 891-900.

CERMAKOVÁ, P., PETERKA, M., CAPKOVÁ, J., TURECKOVÁ, J., RUCH, J.V., LESOT, H. and PETERKOVÁ, R. (1998). Comparison of the tooth shape and size in tabby and non-tabby mice. *Acta Vet. Brno 67*: 3-14.

COHN, S.A. (1957). Development of the molar teeth in the albino mouse. *Am. J. Anat. 101*: 295-320.

COIN, R., LESOT, H., VONESCH, J.L., HAÏKEL, Y. and RUCH, J.V. (1999). Aspects of cell proliferation kinetics of the inner dental epithelium during mouse molar and incisor morphogenesis : a reappraisal of the role of the enamel knot area. *Int. J. Dev. Biol. 43*: 261-268.

CRAWFORD, P.J., ALDRED, M.J. and CLARKE, A. (1991). Clinical and radiographic dental findings in X linked hypohidrotic ectodermal dysplasia. *J. Med. Genet. 28*: 181-185.

FAUSSER, J.L., SCHLEPP, O., ABERDAM, D., MENEGUZZI, G., RUCH, J.V. and LESOT, H. (1998). Localization of antigens associated with adherens junctions, desmosomes and hemidesmosomes during murine molar morphogenesis. *Differentiation 63*: 1-11.

FERGUSON, B.M., BROCKDORFF, N., FORMSTONE, E., NGYUEN, T., KRONMILLER, J.E. and ZONANA, J. (1997). Cloning of Tabby, the murine homolog of the human EDA gene: evidence for a membrane-associated protein with a short collagenous domain. *Hum. Mol. Genet. 6*: 1589-1594.

GREEN, M.C. (Ed.). (1981). *Genetic Variants and Strains of the Laboratory Mouse*. Gustav Fischer Verlag, Stuttgart, New York, pp. 1-476.

GRÜNEBERG, H. (1965). Genes and genotypes affecting the teeth of the mouse. *J. Embryol. Exp. Morphol. 14*: 137-159.

GRÜNEBERG, H. (1966). The molars of the tabby mouse, and a test of the 'single-active X-chromosome' hypothesis. *J. Embryol. Exp. Morphol. 15*: 223-244.

GRÜNEBERG, H. (1971). The tabby syndrome in the mouse. *Proc. R. Soc. Lond. (Biol.) 179*: 139-156.

HU, C.C., SAKAKURA, Y., SASANO, Y., SHUM, L., BRINGAS, P., WERB, Z. and SLAVKIN, H.C. (1992). Endogenous epidermal growth factor regulates the timing and pattern of embryonic mouse molar tooth morphogenesis. *Int. J. Dev. Biol.* 36: 505-516.

ISAACS, K., BROWN, G. and MOORE, G.P. (1998). Interactions between epidermal growth factor and the Tabby mutation in skin. *Exp. Dermatol. 7*: 273-280.

JORGENSON, R.J. (1980). Clinician's view of hypodontia. *J. Am. Dent. Assoc. 101*: 283-286.

KAPALANGA, J. and BLECHER, S.R. (1990). Effect of the X-linked gene Tabby (Ta) on eyelid opening and incisor eruption in neonatal mice is opposite to that of epidermal growth factor. *Development 108*: 349-355.

KERR, J.F.R., GOBÉ, G.C., WINTERFORD, C.M. and HARMON, B.V. (1995). Anatomical methods in cell death. In *Methods in Cell Biology* (Eds. L.M. Schwartz and B.A. Osborne). Academic Press, London, pp. 1-27.

KIEFFER, S., PETERKOVÁ, R., VONESCH, J.L., RUCH, J.V., PETERKA, M., and LESOT H. (1999). Morphogenesis of the lower incisor in the mouse from the bud to early bell stage. *Int. J. Dev. Biol. 43:* 531-539.

KOLLAR, E.J. and BAIRD, G.R. (1969). The influence of the dental papilla on the development of tooth shape in embryonic mouse tooth germs. *J. Embryol. Exp. Morphol. 21*: 131-148.

KOLLAR, E.J. and BAIRD, G.R. (1970). Tissue interactions in embryonic mouse tooth germs. II. The inductive role of the dental papilla. *J. Embryol. Exp. Morphol. 24*: 173-186.

KRONMILLER, J.E., UPHOLT, W.B. and KOLLAR, E.J. (1991a). Expression of epidermal growth factor mRNA in the developing mouse mandibular process. *Arch. Oral Biol. 36*: 405-410.

KRONMILLER, J.E., UPHOLT, W.B. and KOLLAR, E.J. (1991b). EGF antisense oligodeoxynucleotides block murine odontogenesis in vitro. *Dev. Biol. 147*: 485-488.

LESOT, H., PETERKOVÁ, R., SCHMITT, R., MEYER, J.M., VIRIOT, L., VONESCH, J.L., SENGER, B., PETERKA, M. and RUCH, J.V. (1999). Initial features of the inner dental epithelium histo-morphogenesis in the first lower molar in mouse. *Int. J. Dev. Biol. 43:* 245-254.

LESOT, H., VONESCH, J.L., PETERKA, M., TURECKOVÁ, J., PETERKOVÁ, R. and RUCH, J.V. (1996). Mouse molar morphogenesis revisited by three dimensional reconstruction : II). Spatial distribution of mitoses and apoptosis in cap to bell staged first and second upper molar teeth. *Int. J. Dev. Biol. 40:* 1017-1031.

MAAS, R. and BEI, M. (1997). The genetic control of early tooth development. *Crit. Rev. Oral Biol. Med. 8*: 4-39.

MEYER, J.M., RUCH, J.V., KUBLER, M.D., KUPFERLE, C. and LESOT, H. (1995). Cultured incisors display major modifications in basal lamina deposition without further effect on odontoblast differentiation. *Cell Tissue Res. 279*: 135-147.

MILLER, W.A. (1978). The Dentitions of Tabby and Crinkled Mice (an upset in mesodermal:ectodermal interaction). In *Development, Function and Evolution of Teeth* (Eds. P.M. Butler and K.A. Joysey), Academic Press London. pp. 99-109.

NEXO, E, HOLLENBERG, M.D., FIGUEROA, A. and PRATT, R.M. (1980). Detection of epidermal growth factor-urogastrone and its receptor during fetal mouse development. *Proc. Natl. Acad. Sci. USA 77*: 2782-2785.

NSO, M., SENGER, B. and RUCH, J.V. (1992). Scoring mitotic activity in longitudinal sections of mouse embryonic incisors: significant differences exist for labial and lingual inner dental epithelia. *J. Craniofac. Genet. Dev. Biol. 12*: 159-166.

OBARA, N. and TAKEDA, M. (1997). Distribution of the neural cell adhesion molecule (NCAM) during pre- and postnatal development of mouse incisors. *Anat. Embryol. (Berl). 195*: 193-202.

OLIVO, J.C., IZPISUA-BELMONTE, J.C., TICKLE, C., BOULIN, C. and DUBOULE, D. (1993). Reconstruction from serial sections : a tool for developmental biology. Application to Hox genes expression in chicken wing buds. *Bioimaging 1:* 151-158.

OSMAN, A. and RUCH, J.V. (1976). Répartition topographique des mitoses dans l'incisive et la 1ère molaire inférieures de l'embryon de souris. *J. Biol. Buccale. 4*: 331-348.

PALACIOS, J., BENITO, N., BERRAQUERO, R., PIZZARO, A., CANO, A. and GAMALLO, C. (1995). Differential spatiotemporal expression of E- and P-cadherin during mouse tooth development. *Int. J. Dev. Biol. 39:* 663-666.

PETERKOVÁ, R., LESOT, H., VONESCH, J.L., PETERKA, M. and RUCH, J.V. (1996). Mouse molar morphogenesis revisited by three dimensional reconstruction : I) Analysis of initial stages of the first upper molar development revealed two transient buds. *Int. J. Dev. Biol. 40*: 1009-1016.

PETERKOVÁ, R., PETERKA, M., and RUCH, J.V. (1993a). Morphometric analysis of potential maxillary diastemal dental anlagen in three strains of mice. *J. Craniofac. Genet. Dev. Biol. 13*: 213-22.

PETERKOVÁ, R., PETERKA, M., VONESCH, J.L. and RUCH, J.V. (1993b). Multiple developmental origin of the upper incisor in mouse: histological and computer assisted 3-D-reconstruction studies. *Int. J. Dev. Biol. 37*: 581-588.

RANTA, R. (1988). Numeric anomalies of teeth in concomitant hypodontia and hyperdontia. *J. Craniofac. Genet. Dev. Biol. 8*: 245-251.

ROBERTSON, N.W. and BLECHER, S.R. (1987). Epidermal growth factor (EGF) affects sulphydryl and disulphide levels in cultured mouse skin: possible relationship between effects of EGF and of the tabby gene on thiols. *Biochem. Cell Biol. 65*: 658-667.

RUCH, J.V. (1990). Patterned distribution of differentiating dental cells: facts and hypotheses. *J. Biol. Buccale 18*: 91-98.

SALMIVIRTA, K., GULLBERG, D., HIRSCH, E., ALTRUDA, F. and EKBLOM, P. (1996). Integrin subunit expression associated with epithelial-mesenchymal interactions during murine tooth development. *Dev. Dyn. 205*: 104-113.

SCHMITT, R., LESOT, H., VONESCH, J.L. and RUCH J.V. (1999). Mouse odontogenesis *in vitro* : the cap-stage mesenchyme controls individual molar crown morphogenesis. *Int. J. Dev. Biol. 43*: 255-260.

SCHWARTZ, L.M. and OSBORNE, B.A. (Eds.) (1995). *Methods in Cell Biology*. Academic Press, London.

SHAPIRO, S.D. and FARRINGTON, F.H. (1983). A potpourri of syndromes with anomalies of dentition. *Birth Defects 19*: 129-140.

SHUM, L., SAKAKURA, Y., BRINGAS, P. Jr., LUO, W., SNEAD, M.L., MAYO, M., CROHIN, C., MILLAR, S., WERB, Z., BUCKLEY, S., HALL, F.L., WARBURTON, D. and SLAVKIN, H.C. (1993). EGF abrogation-induced fusilli-form dysmorphogenesis of Meckel's cartilage during embryonic mouse mandibular morphogenesis in vitro. *Development. 118*: 903-917.

SOFAER, J.A. (1969a). Aspects of the tabby-crinkled-downless syndrome. I. The development of tabby teeth. *J. Embryol. Exp. Morphol. 22*: 181-205.

SOFAER, J.A. (1969b). Aspects of the tabby-crinkled-downless syndrome. II. Observations on the reaction to changes of genetic background. *J. Embryol. Exp. Morphol. 22*: 207-227.

SOFAER, J.A. (1977). The teeth of the "sleek" mouse. *Arch. Oral Biol. 22:* 299-301.

SOFAER, J.A. (1979). Additive effects of the genes tabby and crinkled on tooth size in the mouse. *Genet. Res. 33*: 169-174.

SRIVASTAVA, A.K., PISPA, J., HARTUNG, A.J., DU, Y., EZER, S., JENKS, T., SHIMADA, T., PEKKANEN, M., MIKKOLA, M.L., KO, M.S., THESLEFF, I., KERE, J. and SCHLESSINGER, D. (1997). The Tabby phenotype is caused by mutation in a mouse homologue of the EDA gene that reveals novel mouse and human exons and encodes a protein (ectodysplasin-A) with collagenous domains. *Proc. Natl. Acad. Sci. USA. 94*: 13069-13074.

THESLEFF, I. and SHARPE, P. (1997). Signalling networks regulating dental development. *Mech. Dev. 67*: 111-123.

TURECKOVÁ, J., LESOT, H., VONESCH, J.L., PETERKA, M., PETERKOVÁ, R. and RUCH, J.V. (1996). Apoptosis is involved in disappearance of the diastemal dental primordia in mouse embryo. *Int. J. Dev. Biol. 40:* 483-489.

VAAHTOKARI, A., ÅBERG, T. and THESLEFF, I. (1996). Apoptosis in the developing tooth: association with an embryonic signaling center and suppression by EGF and FGF-4. *Development 122*: 121-129.

VARGAS, G.A., FANTINO, E., GEORGE-NASCIMENTO, C., GARGUS, J.J. and HAIGLER, H.T. (1996). Reduced epidermal growth factor receptor expression in hypohidrotic ectodermal dysplasia and Tabby mice. *J. Clin. Invest. 97*: 2426-2432.

VIELKIND, U. and HARDY, M.H. (1996). Changing patterns of cell adhesion molecules during mouse pelage hair follicle development. 2. Follicle morphogenesis in the hair mutants, Tabby and downy. *Acta Anat. (Basel) 157*: 183-194.

WARSHAWSKY, H. (1968). The fine structure of secretory ameloblasts in rat incisors. *Anat. Rec. 161*: 211-229.

WEEKS, N.L. and BLECHER, S.R. (1983). Evidence from thiol histochemistry for homology between the Tabby-crinkled syndrome in mice and human ectodermal dysplasia. *J. Histochem. Cytochem. 31*: 1407-1411.

YOSHIBA, K., YOSHIBA, N., ABERDAM, D., MENEGUZZI, G., PERRIN-SCHMITT, F., STOETZEL, C., RUCH, J.V. and LESOT, H. (1998a). Expression and localization of laminin-5 subunits during mouse tooth development. *Dev. Dyn. 211*: 164-176.

YOSHIBA, N., YOSHIBA, K., ABERDAM, D., MENEGUZZI, G., PERRIN-SCHMITT, F., STOETZEL, C., RUCH, J.V. and LESOT, H. (1998b). Expression and localization of laminin-5 subunits in the mouse incisor. *Cell Tissue Res. 292*: 143-149.